ARTICLE TYPE

Zinc-seamed pyrogallol[4]arene dimers as structural components in a two-dimensional MOF

Andrew V. Mossine,[a] Collin M. Mayhan,[a] Drew A. Fowler,[a] Simon J. Teat,[b] Carol A. Deakyne, *[a] and Jerry L. Atwood*[a]

The synthesis of a two-dimensional (2D) metal-organic framework (MOF) is described wherein Zn-seamed pyrogallol[4]arene (PgC_x) nanocapsules are utilized as supramolecular building blocks with 4,4'-bipyridine (bpy) linkers. The choice of linker and of crystallization solvent (DMSO) was guided by
10 electronic structure calculations on the zinc model complexes $Zn(C_2H_3O_2)_2L$, which showed that bpy and DMSO have similar Zn–L binding strengths and that there is little drop-off in binding strength when bpy is bound to a second $Zn(C_2H_3O_2)_2$ moiety. The MOF features unusual coordination geometries at the zinc centres along the nanocapsular periphery when compared to previous examples of zinc-seamed nanocapsules. The change in coordination geometry leads to a compulsory change in the internal volume
15 of the nanocapsule as well as the behaviour of the encapsulated guest molecule. There are also several well defined voids and channels within the structure.

1. Introduction

Pyrogallol[4]arenes (PgC_xs), are the pyrogallol-based members of the family of macrocycles known as calixarenes, so named for
20 their resemblance to a "calyx" or cup. The lower rim of the cup is typically hydrophobic in PgC_xs, while the upper rim is hydrophilic due to the presence of twelve hydroxyl groups. These hydroxyls can participate in both inter- and intramolecular hydrogen bonds, making these molecules valuable to the field of
25 supramolecular chemistry as supramolecular building blocks. Depending on the solvent system and the presence (or absence) of heteromolecules, PgC_xs can self-assemble into a variety of structural motifs, including capsules, tubes, and layered structures, among others.[1-7]

30 In addition to participating in non-covalent interactions, PgC_xs can participate in coordinative bonding with transition metal ions and, as a result, form metal–organic nanocapsules (MONCs). Formation of dimeric and/or hexameric MONCs has been reported *via* coordination of PgC_xs to Cu^{2+}, Zn^{2+}, Co^{2+}, Ni^{2+}, and
35 Ga^{3+} (Fig. 1).[8-11] Research emphasis has traditionally been placed on the synthesis of new capsules and/or control over the type of capsule (dimeric or hexameric) that is formed.[12-17] Control over the exterior of the MONC, however, has received much less attention.[18, 19] Both dimeric and hexameric MONCs bear a large
40 number of metal ions on their exterior, each usually capped by a single external ligand. As such, these MONCs are ideal candidates to explore as building blocks in the construction of metal-organic frameworks (MOFs). The first reported PgC_x MONC was synthesised *via* coordination of 6 hydroxyl-footed
45 PgC_{3OH} macrocycles to 24 Cu^{2+} centres.[20] Interestingly, refinement of the crystal structure revealed that some of the
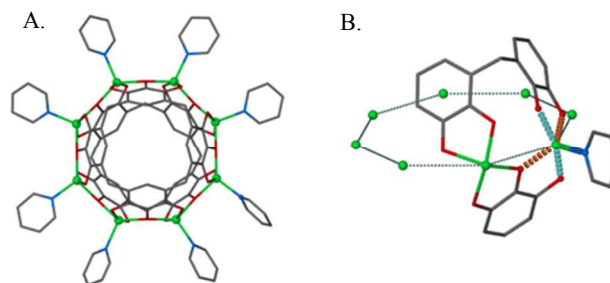
Fig. 1: A) Zinc-seamed nanocapsule (**1**) viewed perpendicular to its "octametal belt." B) Illustration of the angles used in τ5 angular analysis
50 (τ5= Θ_1- Θ_2/60). Θ_1 is the O-Zn-O angle indicated by the turquoise bonds whereas Θ_2 is indicated by the orange bonds. Internal guest and hydrogen atoms are removed for clarity.

terminal hydroxyl groups from the "tails" of each hexameric MONC coordinate to Cu^{2+} centres on neighbouring hexamers,
55 thus forming a 1D coordination polymer.[20] Inspired by this finding, we recently investigated the copper-seamed dimeric MONC as a building block towards the construction of MOFs and successfully linked individual dimers through two radically different modes of coordinative bonding into 1D chains.[18] Ideally,
60 control over dimensionality is achievable but, thus far, attempts to synthesise linked arrays of Cu-seamed dimers of a higher dimensionality (i.e., 2- or 3-dimensional MOFs) have been unsuccessful. Thus, alternate methods have been explored to form multidimensional linked arrays of PgC-based MONCs.

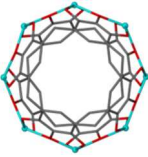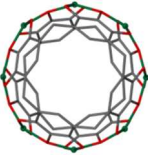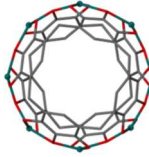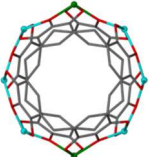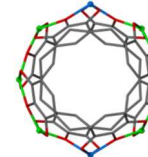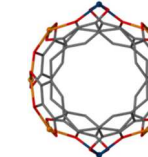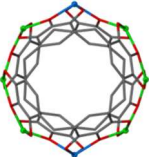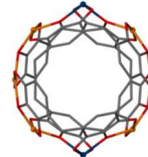65 Structural analysis of previously published dimeric MONCs shows that dimers generated from different transition metals display clear differences in their coordination environments.[18] The variations in the lengths and angles of the phenolic-metal

ARTICLE TYPE

Table 1 Examples of dimeric metal-seamed pyrogallol[4]arene capsules bearing five and six-coordinate metal sites.

Assembly	PgC₃ZnDMSO (1)	PgC3CuDMSO	PgC₁Cu4,4'-bpy	PgC₁Zn4,4'-bpy(2)			PgC₂CoPy			PgC2NiPy		
Metal Centre	**Zn (average)**	**Cu (average)**	**Cu (average)**	**Zn1**	**Zn2**	**Zn3**	**Co1**	**Co2**	**Co3**	**Ni1**	**Ni2**	**Ni3**
Angle 1 (°)	162 ± 1	172 ± 1	171 ± 1	170	166	156	173	169	157	179	170	159
Angle 2 (°)	137 ± 1	152 ± 1	151 ± 2	148	139	121	149	139	120	168	145	110
τ5	0.42 ± 0.03	0.33 ± 0.01	0.33 ± 0.01	0.37	0.45	n/a	0.40	0.51	n/a	0.18	0.43	n/a
Coordination #	5	5	5	5	5	6	5	5	6	5	5	6

[a] Angles used for τ5 calculations along with the resultant τ5 values are listed, as well as the coordination numbers of the metals along the capsular periphery. [b] Compounds **1** and **2,** which are described in the text, are located at the far left and third from right, respectively. [c] All dimers are shown perpendicular to the plane of the equatorial "octametal belt."

5 bonds that seam the dimers together are visually apparent when dimers comprising different transition metals are compared (Table 1)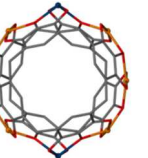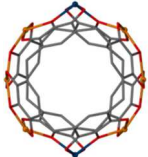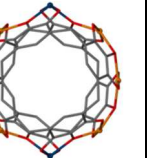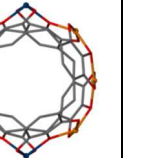. A more quantitative measure of these differences is the τ5 value (Fig. 1b), a 0-1 scale that describes the tendency of a distorted penta-coordinate metal center to approach a square 10 pyramidal (0) versus a trigonal bipyramidal (1) geometry.[21] Thus, the τ5 value is a simple numerical method by which a wide assortment of penta-coordinate species may be compared. Analysis of τ5 for various metal-seamed dimers shows a significant deviation in the value for the zinc-seamed 15 pyrogallol[4]arene dimer (**1**) compared to that of its copper-seamed analogue (Table 1). It was therefore hypothesized that if a MOF could be generated from zinc-seamed dimers, it would likewise be geometrically different from our previously reported copper-based assembly.

20 Our interest in the zinc-seamed dimeric assembly was significantly strengthened by the pioneering work of Power et al. that demonstrated that ligands around the periphery of **1** could be exchanged without compromising its structural integrity.[19] Thus, given an appropriate linking molecule that could displace other 25 ligands, **1** could easily be envisioned to act as a building block in the construction of MOFs, much like the copper-seamed dimer. Due to our previous success with 4,4'-bipyridine (bpy) with the copper-seamed dimer,[18] as a further test of our hypothesis, quantum chemical calculations were performed on mononuclear 30 zinc model complexes to assess the affinity of bpy as a tethering ligand for the zinc-seamed dimeric nanocapsules. The computational results further spurred our attempt to synthesize a tethered capsular assembly.

2. Computational and Experimental Details

2.1 Computational details

In earlier quantum chemical calibration studies, we examined zinc complexes composed of combinations of hydroxide, water 40 and solvent ligands (e.g., $Zn(OH)_2(H_2O)_2L_{1,2}$) or deprotonated (Z)-ethene-1,2-diol and solvent molecules ($Zn(C_2O_2H_3)_2L$) as possible mononuclear zinc models for the metal centres in PgC_xZn dimers such as **1**.[22, 23] The solvent ligands L included C_5H_5N, NH_3, CH_3OH, $(CH_3)_2NCHO$ and $(CH_3)_2SO$. Although 45 optimization of the hydroxide-containing models yielded mainly 4-coordinate zinc complexes with outer-shell hydrogen-bonded networks, optimization of the $Zn(C_2O_2H_3)_2L$ complexes yielded 5-coordinate zinc complexes with average Zn–X bond lengths and X–Zn–Y bond angles within the ranges observed 50 experimentally for the zinc-seamed PgC nanocapsules.[9, 24]

With the success of the $Zn(C_2O_2H_3)_2$ models in reproducing the zinc-coordination environment of the dimeric nanocapsules and the trends in relative ligand bond dissociation enthalpies (BDEs), these models were implemented in our study of bpy as a 55 possible tethering ligand for the zinc-seamed capsules. On the basis of the calibration results, fully optimized geometries and normal-mode vibrational frequencies were computed for $Zn(C_2O_2H_3)_2$bpy and $(Zn(C_2O_2H_3)_2)_2$bpy at the M05-2X/B2-PP level of theory. The notation B2-PP designates a basis set with 60 the small-core Stuttgart/Dresden pseudopotential on Zn, with scalar relativistic effects included. The B2 basis set is [10s7p4d3f] for Zn and 6-311+G(2df,2p) for the remaining atoms.[25] The geometries were optimized with the keywords opt = tight and int = ultrafine. Starting geometries had a square 65 pyramidal arrangement of the zinc ligands, with the C–H bonds of the bpy placed over the O⁻group of a given $C_2O_2H_3^-$. In all of our earlier work, starting with a trigonal bipyramidal arrangement led to optimized structures closer to square pyramidal and orienting the C–H bond over the O⁻ maximized the C–H···O 70 interaction.
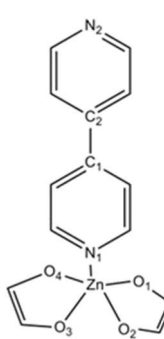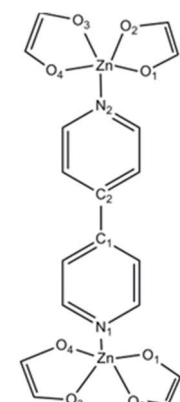
The normal-mode vibrational frequencies were computed to confirm the presence of minima (no imaginary frequencies) and

Journal Name

Chemical Science

ARTICLE TYPE

Table 2 Energetic and geometric properties of($Zn(C_2O_2H_3)_2)_{1,2}$ bpy complexes.

Complex	$Zn(C_2O_2H_3)_2$bpy	$(Zn(C_2O_2H_3)_2)_2$bpy
BDEs^a (kJ/mol)	95.7 (55.6)	92.3 (49.5)
Bond Lengths (Å)^b	Zn–O$_{avg}$: 2.069 (1.923– 2.212)	Zn–O$_{avg}$: 2.066 (1.920– 2.211)
	Zn–N: 2.071	Zn–N: 2.079
Bond Angles (°)	O$_1$–Zn–O$_3$: 162.1	O$_1$–Zn–O$_3$: 164.0
	O$_2$–Zn–O$_4$: 145.1	O$_2$–Zn–O$_4$: 147.1

^{a} MP2/B2-PP//M05-2X/B2-PP results in kJ/mol. ΔH_{298} and ΔG_{298} (in parentheses) binding dissociation data. ^{b} Range of Zn–O bond lengths in parentheses. The experimentally observed ranges for these geometric parameters are : Zn–O = 2.01 – 2.11 Å; Zn–N = 2.01 – 2.07 Å ; O –Zn–O = 79 – 170°.

to convert energy differences to enthalpy and free energy differences. To improve the energetics, single-point energies were evaluated at the MP2/B2-PP//M05-2X/B2-PP level of theory.[22, 23] All calculations were performed with use of the Gaussian 09 package.[26]

2.2 Experimental details

All reagents were purchased from commercial sources and were used as received. The rccc "cone" conformer of the *C*-methylpyrogallol[4]arene (PgC$_1$) macrocycle was synthesized, purified, and characterized as previously described.[18] Dimeric zinc-seamed MONC **1** was also synthesized in a manner that was similar to, but slightly different from, published methods.[9] A solution of PgC$_1$ was added to an acetonitrile solution of Zn(NO$_3$)$_2$ and pyridine. The resultant yellow precipitate (**1**) was removed *via* vacuum filtration, dried in a dessicator overnight and used without further purification. This material was dissolved in hot dimethyl sulfoxide (DMSO), typically at a 10^{-2} M concentration, and mixed with a DMSO solution of bpy, in a ratio of 2.5 bpy per **1**. On cooling, small yellow crystals grew over a period of several hours to several days, depending on the concentrations of the reagents. Crystals grown using different ratios of bpy to **1** were in all likelihood isostructural, as they did

not differ in their unit cell parameters. Alternately, the same material (i.e. with identical unit cell parameters) could be formed *via* direct synthesis, wherein PgC$_1$, Zn(NO$_3$)$_2$, pyridine and bpy were mixed in a hot DMSO solution, with crystal formation apparent upon cooling. A 1:4:12:x PgC$_1$:Zn(NO$_3$)$_2$:pyridine:bpy reagent ratio was used for direct synthesis, with x=1-5. Pyridine-free direct synthesis was also possible, but necessitated a higher proportion of bpy (i.e., 1:4:4-8 PgC$_1$:Zn(NO$_3$)$_2$:bpy). The single crystal X-ray diffraction data for this material was collected on Station 11.3.1 of the Advance Light Source using a Bruker APEX II CCD diffractometer at a wavelength of 0.77490 Å and a temperature of 100(2) K.

3. Results and Analysis of Results

The M05-2X/B2-PP equilibrium structures for bpy and the $(Zn(C_2O_2H_3)_2)_{1,2}$bpy complexes show that the D$_2$ symmetry of bpy is preserved for the $(Zn(C_2O_2H_3)_2)_2$bpy complex, but the symmetry lowers to C$_2$ for $Zn(C_2O_2H_3)_2$bpy. Also, the dihedral angle that determines the canting between the two pyridines in bpy differs by less than 2° between the lone ligand and the ligated species. The τ5 values for the zinc centre(s) in the zinc model complexes are both 0.28, reflecting the greater flexibility of the

ARTICLE TYPE
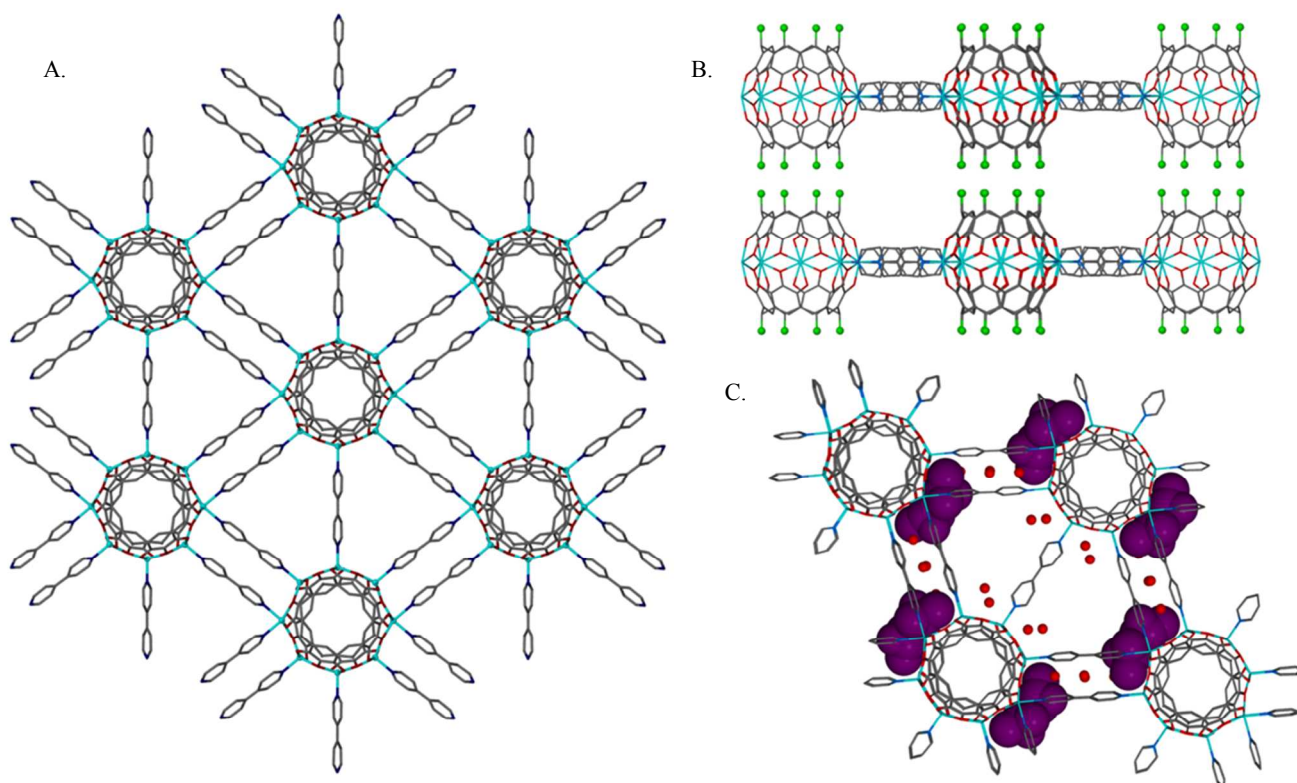
Fig. 2 View of MOF **2** along the crystallographic c axis and a axis, respectively (A, B). C-methyl groups of the pyrogallol[4]arene macrocycle shown in green. Arrangement of solvent within the superstructure: ordered DMSO molecules are shown in violet and disordered solvent is shown in red (C).

model versus the capsule (Tables 1 and 2).[9, 24] This overemphasized square pyramidal character is likely due to the absence of the bridging hydrogen(s) and adjacent zinc centres, which would have a constraining effect on the structure. Even though the calculated τ5 values differ by 0.1 – 0.2 from experiment, the O–Zn–O bond angles used to calculate τ5 are within 6° of the O–Zn–O bond angles of Zn1 of **2** (Table 2).

The MP2/B2-PP//M05-2X/B2-PP results for the binding enthalpies and free energies between a bpy and one or two $Zn(C_2O_2H_3)_2$ complexes are reported in Table 2. The BDE of bpy to a second zinc complex exhibits minimal drop-off (3.4 kJ/mol) in comparison to the BDE of bpy to the first zinc complex (Table 2). This independence of the individual zinc-bpy coordination instances suggests that linking of zinc-seamed dimer capsules indeed can be achieved. The BDE of bpy (95.7 kJ/mol) is essentially equal to those of pyridine (96.6 kJ/mol) and DMSO (96.5 kJ/mol) calculated at the same level of theory.[22, 23] These relative BDEs aided in the choice of DMSO as the solvent for synthesis and crystallization. It was found that the more competitive the binding affinities of the external ligand and solvent, the slower and more effective the crystallization process.

Structural refinement of the single crystal X-ray diffraction data reveals that the result of the previously described syntheses

is a novel two-dimensional MOF (**2**, Fig. 2). The asymmetric unit contains one half of a PgC_1 macrocycle along with three metal centres, one at full occupancy and two at half occupancy, each bearing one half of a bpy ligand. Structural expansion shows a complete dimeric capsule coordinatively linked to six adjacent dimers *via* ten bpy ligands. Each dimer is connected to two of its neighbours *via* a single bpy unit, and to the other four by two bpy units. Unit cell expansion along the *a* and *b* crystallographic axes shows that the long-range order of the structure exhibits a centred hexagonal lattice with the interstitial space between dimers and bpy linkers partially occupied by solvent molecules. Of these, one crystallographically unique and ordered DMSO molecule lies on the periphery above and below pairs of bpy molecules (Fig. 2c). Additional structural units, modelled as disordered water molecules, occupy the space within two adjacent triangular portals between dimers, as well as among linker molecules. Interestingly, unit cell expansion along the *c* axis shows that parallel layers of **2** stack in a perfect AA layer arrangement, perhaps due to favourable van der Waals interactions between *C*-methyl groups on adjacent dimers (3.73 and 3.76 Å C-C distances between *C*-methyls on adjacent dimers, Fig. 2b). The direct consequence of this stacking pattern is the formation of a network of channels that propagates throughout the structure, notably

Journal Name
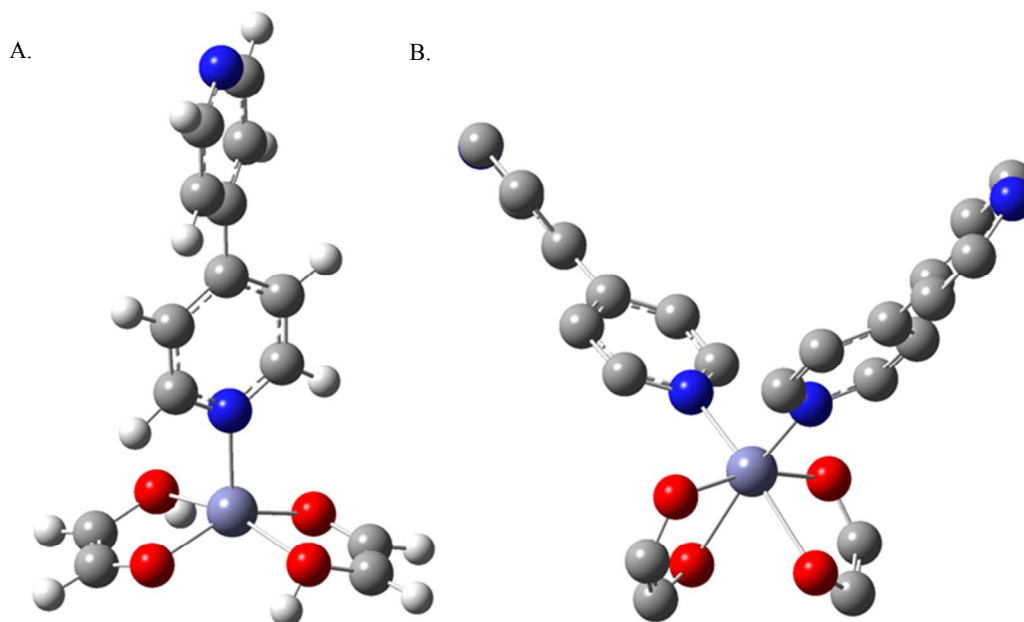
Chemical Science

ARTICLE TYPE
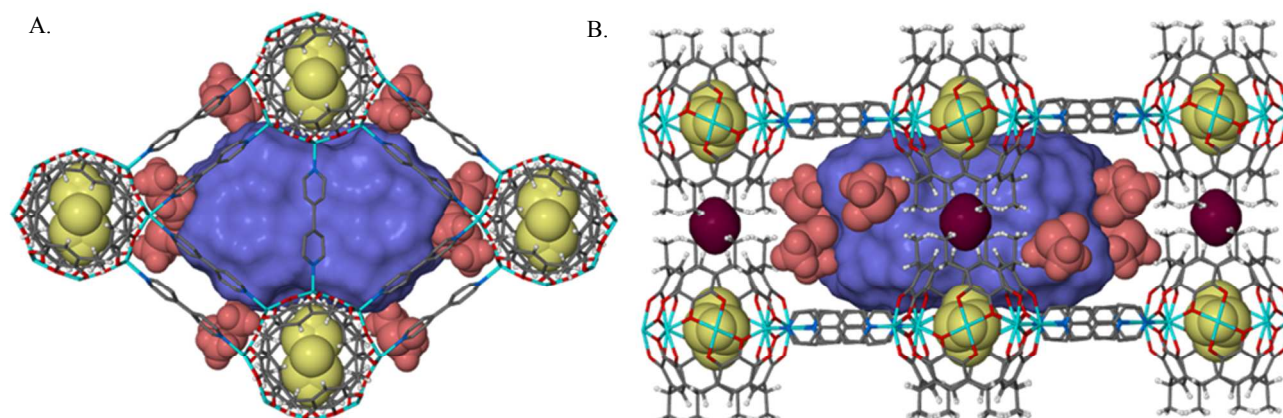
Fig. 3 Image of the volume contained within a pair of triangular portals (violet) along the A) c axis and B) a axis. Smaller voids (maroon) are present between pendant C-methyl chains of the dimers. Incarcerated (yellow) and structural (red) DMSO molecules are also shown.

Fig. 4 M05-2X/B2-PP optimized structures of the A.) $Zn(C_2O_2H_3)_2bpy$ complex. B.) $Zn(C_2O_2H_3)_2(bpy)_2$ complex. Hydrogens removed for clarity.

along the *c* axis. This is due to the stacking of the aforementioned triangular portals, which are largely devoid of structural building blocks and contain highly disordered solvent molecules. In addition to being connected to one another along the *c* axis, these triangular channels also appear to be interconnected along the *a* and *b* axes, at junctions between individual MOF layers. However, these regions also contain ordered solvent molecules, so it is uncertain whether these regions are truly connected to one another in a solvated crystal.

In the interest of using this assembly for molecular sorption/ separation studies, it was important to determine the void volumes contained within the structure. Of specific interest were the triangular portals, as, with an area of 143.5 $Å^2$ per layer, these are the largest and most easily defined free space-containing motifs found in the structure. Because the portals are not spatially finite, the volume contained within a pair in a single layer was calculated by blocking them at their borders prior to volume analysis using MSRoll with X-Seed as the interface.[27, 28] This treatment gave an accessible volume of 705 $Å^3$ per triangular pair with a probe radius of 1.25 Å (Fig. 3). Thus, a single repeating triangular unit of this portal encloses an overall volume of approximately 352 $Å^3$ per layer, large enough to accommodate a variety of guest species. Unexpectedly, MSRoll also revealed the presence of additional voids within the structure, located between

the pendant *C*-methyl arms of adjacent nanocapsules (Fig. 3b). These voids are significantly smaller, with a contact volume of 42 Å^3 and an accessible volume of only 4 Å^3 once calculated methyl hydrogens are included in the structure. As such, these voids are [5] unlikely to be useful in the entrapment/storage of any but the smallest of guest species.

To enable formation of this unique MOF, the coordination geometry of the zinc centres is drastically altered as compared to that in **1.** As each dimer accommodates a total of ten peripheral [10] ligands, two more than seen prior to linking, a change in the coordination number of two Zn centres from 5 to 6 is necessary. The geometry of the other six zinc centres is altered to compensate for this distortion, as is the framework's normally spherical shape. One particular outcome of this is an increase in [15] the capsule's molecular volume, from previously published values of 141 Å^3 and 143 Å^3 in **1** to 147 Å^3 in **2**.[9, 24] Despite the distortion in the O–Zn-O bond angles caused by the presence of the six-coordinate zincs, the Zn–O (2.01 – 2.08 Å) and Zn–N (2.04 – 2.07 Å) bond lengths of the five-coordinate zincs are [20] within the ranges observed by Power et al. for **1** and the corresponding capsule with pyridine ligands (2.01 – 2.09 Å).[9] The Zn–O$_{avg}$ and Zn–N bond lengths obtained from the quantum chemical calculations are in good agreement with the experimental results (Table 2). When a second bpy ligand is [25] coordinated to a [Zn(C$_2$O$_2$H$_3$)$_2$bpy] complex, the resulting M05-2X/B2-PP equilibrium structure has a distorted octahedral coordination environment around the zinc (Fig. 4), with slightly more distortion than is seen experimentally. The structural reproducibility is further evidence that instructive results can be [30] obtained from these relatively simple model complexes.

Interestingly, the change in coordination geometry also affects the internal DMSO guest. In other examples of guest encapsulation within a dimer, where each metal centre is penta-coordinate, the guest tends to be badly disordered over multiple [35] possible positions (Fig. 5a).[9, 16] This is partially due to the fact that coordinating guests, such as pyridine and DMSO can loosely coordinate to all eight of the metal centres in a dimer, as each penta-coordinate metal centre is equally likely to accommodate an additional ligand. This mode of internal coordination, [40] however, is not possible in **2**. As two of the zinc centres in **2** are formally hexa-coordinate, they cannot accommodate additional ligand binding from the interior. This causes the internal guest DMSO to instead be directed toward the remaining penta-coordinate centres, reducing guest disorder and allowing the [45] DMSO molecule to be modelled over four discrete positions (Fig. 5b). This suggests that control over the coordination number of the metal centres in PgC-based dimers, if possible, can be used to control the behaviour of the internal guest, an idea that has yet to be thoroughly explored.

[50] To quantify the distortion that is introduced by this aberrant coordination geometry, τ5 values were calculated for the two crystallographically unique penta-coordinate zinc centres in **2.** At 0.37 and 0.45, these values differ significantly from one another, as well as from that of previously reported zinc dimers, where the [55] metal centres average at 0.42 with minimal deviation (Table 1). In our previous report with directly-linked copper dimers, steric hindrance around the site of linking necessitated the presence of square planar sites on the capsular periphery.[18] This, in turn,
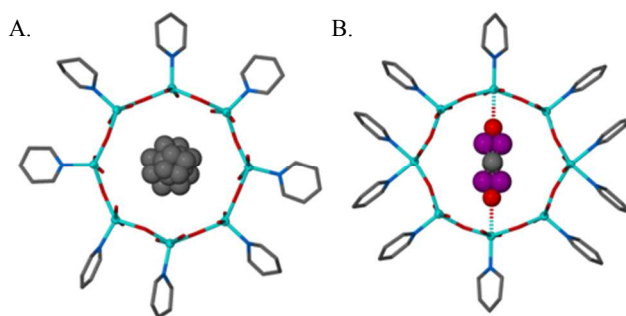
[60] **Fig. 5** Comparison of the guest behaviour in **1** (A.) and **2** (B.). Pyridine guest in **1** is fully disordered (grey) while DMSO guest in **2** is directed away from hexa-coordinate zinc sites, leading to decreased guest disorder.

induced a change in the coordination geometry of nearby penta-coordinate sites to compensate for this geometric disruption. [65] Likewise, the octahedral sites in **2** likely place strain on the spherical framework, thereby forcing geometric compensation by the other metal centres. Thus, this coordinative discrepancy in the penta-coordinate centres may not be due to the use of bpy ligands per se, but rather to the structural constraints enforced by the [70] hexa-coordinate centres. Corroboration for this conclusion can be found with the previously reported copper-seamed bpy linked dimers, where replacing DMSO ligands for bpy ligands did not lead to a significant change in τ5 or a change in coordination number (Table 1). In addition, this conclusion is also supported [75] by our previous work with Co- and Ni-seamed dimers.[10] Although these dimers were synthesized to bear monodentate pyridine ligands, they were nevertheless found to harbour octahedral sites. This observation further suggests that coordination geometry, rather than ligand identity, is responsible [80] for structural distortion.

4. Conclusion

In conclusion, we have shown that zinc-seamed dimers can be used as building blocks in creating a MOF-like array by using divergent ligands commonly used as linkers in more typical [85] MOFs. Electronic structure calculations were used as a proof of principle in our endeavours and spurred us to use bpy as a ligand, akin to our previous work with copper-seamed dimers. The thermochemical data calculated for bpy can provide benchmark values to identify other ligand linker candidates. The zinc-seamed [90] MOF is drastically different from our copper-seamed MOF in both its coordinative and linking geometries. The reason for the difference between the two structures is unknown, but likely has to do with differences in the initial coordinative geometries of the two dimers and the chemical properties of the two respective [95] metals. Furthermore, the structure reported here is significantly more interesting for gas sorption studies, as it features rigid channels that may be useful for gas sorption/separation.

Acknowledgements

Notes and references

[a] *Department of Chemistry, University of Missouri-Columbia,*
5 *Columbia, MO 65211, USA. E-mail: DeakyneC@missouri.edu*
atwoodj@missouri.edu
[b] *Lawrence Berkeley National Laboratory, 1 Cyclotron Road,*
Berkeley, CA 94720, USA. E-mail: sjteat@lbl.gov

10 † Crystal data for PgC$_1$Zn 4,4'-bipyridine (**2**): C$_{29.50}$H$_{21.50}$N$_{2.50}$O$_{7.50}$S$_{0.50}$Zn$_2$, M = 677.76, yellow prism, 0.10 × 0.05 × 0.05 mm^3, orthorhombic, space group *Pban* (No. 50), a = 20.780(2), b = 34.908(4), c = 14.4254(15) Å, V = 10464.3(19) Å^3, Z = 8, D_c = 0.860 g/cm^3, F_{000} = 2752, Bruker Apex II CCD diffractometer, synchrotron radiation, λ = 0.77490 Å, T = 100(2)K,
15 $2\theta_{max}$ = 45.7º, 49286 reflections collected, 5514 unique (R$_{int}$ = 0.0759). Final *GooF* = 1.514, *R1* = 0.1053, *wR2* = 0.3531, *R* indices based on 3603 reflections with I >2sigma(I) (refinement on F^2), 497 parameters, 134 restraints. Lp and absorption corrections applied, μ = 1.213 mm^{-1}.

20
1.   L. Avram, Y. Cohen and J. Rebek, Jr., *Chemical Communications (Cambridge, United Kingdom)*, 2011, **47**, 5368-5375.
2.   O. V. Kulikov, M. M. Daschbach, C. R. Yamnitz, N. Rath and
25   G. W. Gokel, *Chemical Communications (Cambridge, United Kingdom)*, 2009, 7497-7499.
3.   D. A. Fowler, S. J. Teat, G. A. Baker and J. L. Atwood, *Chemical Communications (Cambridge, United Kingdom)*, 2012, **48**, 5262-5264.
30 4.   A. V. Mossine, H. Kumari, D. A. Fowler, A. Shih, S. R. Kline, C. L. Barnes and J. L. Atwood, *Chemistry - A European Journal*, 2012, **18**, 10258-10260, S10258/10251-S10258/10114.
5.   A. V. Mossine, H. Kumari, D. A. Fowler, A. K. Maerz, S. R.
35   Kline, C. L. Barnes and J. L. Atwood, *Israel Journal of Chemistry*, 2011, **51**, 840-842.
6.   S. J. Dalgarno, G. W. V. Cave and J. L. Atwood, *Angewandte Chemie, International Edition*, 2006, **45**, 570-574.
7.   S. J. Dalgarno, J. Antesberger, R. M. McKinlay and J. L.
40   Atwood, *Chemistry - A European Journal*, 2007, **13**, 8248-8255.
8.   S. J. Dalgarno, N. P. Power, J. E. Warren and J. L. Atwood, *Chemical Communications (Cambridge, United Kingdom)*, 2008, 1539-1541.
45 9.   N. P. Power, S. J. Dalgarno and J. L. Atwood, *New Journal of Chemistry*, 2007, **31**, 17-20.
10.   J. L. Atwood, E. K. Brechin, S. J. Dalgarno, R. Inglis, L. F. Jones, A. Mossine, M. J. Paterson, N. P. Power and S. J. Teat, *Chemical Communications (Cambridge, United Kingdom)*,
50   2010, **46**, 3484-3486.
11.   R. M. McKinlay, P. K. Thallapally and J. L. Atwood, *Chemical Communications (Cambridge, United Kingdom)*, 2006, 2956-2958.
12.   P. Jin, S. J. Dalgarno, J. E. Warren, S. J. Teat and J. L.
55   Atwood, *Chemical Communications (Cambridge, United Kingdom)*, 2009, 3348-3350.
13.   A. K. Maerz, H. M. Thomas, N. P. Power, C. A. Deakyne and J. L. Atwood, *Chemical Communications (Cambridge, United Kingdom)*, 2010, **46**, 1235-1237.
60 14.   H. Kumari, R. Kline Steven, J. Schuster Nathaniel and L. Atwood Jerry, *Chem. Commun. (Cambridge, U. K.)* 2011, **47**, 12298-12300.
15.   H. Kumari, R. Kline Steven, G. Wycoff Wei, L. Paul Rick, V. Mossine Andrew, A. Deakyne Carol and L. Atwood Jerry,
65   *Angewandte Chemie (International ed. in English)*, 2012, **51**, 5086-5091.
16.   H. Kumari, A. V. Mossine, S. R. Kline, C. L. Dennis, D. A. Fowler, S. J. Teat, C. L. Barnes, C. A. Deakyne and J. L. Atwood, *Angewandte Chemie, International Edition*, 2012, **51**,
70   1452-1454, S1452/1451-S1452/1203.
17.   H. Kumari, R. Kline Steven, J. Schuster Nathaniel, L. Barnes Charles and L. Atwood Jerry, *Journal of the American Chemical Society*, 2011, **133**, 18102-18105.
18.   D. A. Fowler, A. V. Mossine, C. M. Beavers, S. J. Teat, S. J.
75   Dalgarno and J. L. Atwood, *Journal of the American Chemical Society*, 2011, **133**, 11069-11071.
19.   P. Power Nicholas, J. Dalgarno Scott and L. Atwood Jerry, *Angewandte Chemie (International ed. in English)*, 2007, **46**, 8601-8604.
80 20.   R. M. McKinlay, G. W. V. Cave and J. L. Atwood, *Proceedings of the National Academy of Sciences of the United States of America*, 2005, **102**, 5944-5948.
21.   A. W. Addison, T. N. Rao, J. Reedijk, J. Van Rijn and G. C. Verschoor, *Journal of the Chemical Society, Dalton*
85   *Transactions: Inorganic Chemistry (1972-1999)*, 1984, 1349-1356.
22.   C. M. Mayhan, T. J. Szabo, J. E. Adams and C. A. Deakyne, *Computational & Theoretical Chemistry*, 2012, **984**, 19-35.
23.   C. M. Mayhan, T. J. Szabo, J. E. Adams and C. A. Deakyne,
90   *Structural Chemistry*, 2013, **24**, 2089-2099.
24.   N. Power, S. J. Dalgarno and J. L. Atwood, *Angewandte Chemie, International Edition*, 2007, **46**, 8601-8604.
25.   E. A. Amin and D. G. Truhlar, *Journal of Chemical Theory and Computation*, 2008, **4**, 75-85.
95 26.   M. J. Frisch, et. al., Wallingford CT, 2009.
27.   M. L. Connolly, *Journal of Molecular Graphics*, 1993, **11**, 139-141.
28.   L. J. Barbour, *Journal of Supramolecular Chemistry*, 2003, **1**, 189-191.
100